

Biomimetic Nanomaterials via in situ Synthesis of Atomically-Thin Gold Sheets and Platinum Nanoclusters

M. McTaggart **, M. Jugroot * and C. Malardier-Jugroot **

*Royal Military College of Canada, Dept. of Aero. and Mech. Eng. Kingston, ON

**Royal Military College of Canada, Dept. of Chem. and Chem. Eng.
Kingston, ON, cecile.malardier-jugroot@rmc.ca

ABSTRACT

This paper presents the synthesis and activity of broadly stable polymer-metal nanoreactors capable of confinement-enhanced catalysis. Poly(styrene-*alt*-maleic acid), SMA, is known to self-assemble in water into highly organized supramolecular nanostructures containing polar and non-polar reaction spaces. We use this polymer architecture to direct the reduction of hydrophobic salt precursors into metal nanoclusters under ambient conditions and without extraneous reductant. Small-angle neutron scattering and transmission electron microscopy reveal the gold and platinum nanocatalysts remain embedded within respective hydrophobic and hydrophilic confinement spaces.

Keywords: biomimetics, catalysis, gold nanocrystals, self-assembly, supramolecular materials

1 INTRODUCTION

Many important chemical processes and advanced material classes remain impractical or expensive outside of laboratory scales due to their thermodynamic or kinetic unfavourability [1]. The fixation of atmospheric gases into useable chemicals or the controlled synthesis of functionally complex molecules are two examples of industrially relevant and technologically challenging research areas [1-3]. Yet even the simplest living organisms efficiently promote these processes and indeed make them among the most common chemical reactions on Earth.

A promising approach to understanding Nature's success is to examine the structures responsible for the high reaction efficiency, namely enzymes [4,5]. Enzymes are biological nanoreactors which comprise a macromolecular superstructure and a catalytic active centre. The two elements work in concert: the protein structure reduces the entropic cost of synthetic reactions by increasing the concentration of target substrates within confined reaction sites, and the active center increases reaction kinetics by catalytic control of substrate geometry[5].

Biomimicry can be attempted either through the direct imitation of enzyme structure using chains of amino acids, or by reproducing the physical and chemical properties in other materials. By taking the latter approach, robust nanoreactors could be produced that, unlike natural enzymes, are tolerant to changes in pH, ionic strength, and

temperature that may be encountered in industrial environments [5].

The amphiphilic nanostructure selected for development of a confinement system is composed of self-assembling chains of poly(styrene-*alt*-maleic acid), SMA. In neutral water, internal hydrogen bonding along the SMA polymer produces a rigidly linear backbone chain [6]. Self assembly occurs because the enthalpy gain from minimizing the contact area of the styrene groups with water is greater than the entropic cost of association [7].

Small angle neutron scattering (SANS) provides a unique approach for the investigation of the association of polymers because this method allows for characterization in solution. A very high contrast between the deuterated solvent and the hydrogenated polymer allows the size and shape of the nanoarchitecture to be elucidated by fitting the SANS spectrum with characteristic models. A hollow cylinder form factor revealed that SMA self-assembles into nanotubes with 28Å interior and 41Å exterior diameters.

Characterization of the association of high molecular weight SMA shows that the individual chain conformation remains the same as that observed in previous [8] studies of SMA self-assembly but while low molecular weight chains form nanotubes, longer chains instead associate into bi-layer sheets with similar interior dimension [6,7,9]. In both low and high molecular weight cases, the structures' interior spaces have primarily hydrophobic surfaces while the exterior is primarily hydrophilic [10].

This paper presents the synthesis and characterization of noble metal nanocrystalization into active centres within confined reaction sites of a supramolecular, self-assembling polymeric nanostructure. Metal species-specific nanocrystal formation is observed within hydrophobic and hydrophilic confinement areas, making for a highly tunable and versatile reactor system.

2 EXPERIMENTAL

Poly(styrene-*alt*-maleic anhydride), partial methyl-ester (350, 000 mw avg, Sigma-Aldrich) was dissolved in water to form a 1% wt/wt solution and neutralized to pH 7 with NaOH. Noble metal SMA solutions were produced by adding 0.0358g platinum(II) chloride (PtCl₂, 98%, Sigma-Aldrich) or 0.0347g gold(I) chloride (AuCl, 99.9%, Sigma-Aldrich) to 3mL SMA solution and mixing by sonication

for 1.5 hours. D₂O and NaOD were used for small angle neutron scattering (SANS) experiments.

Molecular modeling was completed using Gaussian09 software [11]. Metal-polymer interactions were simulated with a three part ONIOM model: the outer monomers were modeled at the semi-empirical PM6 level of theory; the central monomer was modeled using density functional theory (DFT) B3PW91 functional and 6-31G basis set; metal atoms were modeled using DFT B3PW91/LANL2DZ. This splitting has been shown to give high quality results for simulations of transition metal interactions with oxygen and benzene complexes [12].

SANS experiments were performed on the NG3-30m instrument at the NIST Center for Neutron Research, Gaithersburg, MD, using an incident wavelength of 6Å at sample to detector distances of 1.00, 6.00, and 13.00m. Raw data was reduced at NIST-CNR using the Igor Macros package. Analysis of the reduced data was performed using SasView 3.0.0 (<http://www.sasview.org>).

Transmission electron microscopy (TEM) experiments were performed at the Canadian Centre for Electron Microscopy, McMaster University, Hamilton, ON, using a high-resolution FEI HR-TEM/STEM Titan 80-300LB microscope operating at 300kV.

3 RESULTS AND DISCUSSION

An overview of the noble metal and SMA nanoreactor system, including its catalytic activity, is detailed in Section 3.1. Section 3.2 contains a thorough characterization of the Pt-SMA system through molecular modeling, SANS, and TEM. The metal salt reduction method is expanded to gold(I) chloride in Section 3.3.

3.1 Nanoreactor structure and function

The supramolecular SMA polymer provides the structure for the nanoreactors under development. Non-polar molecules, including hydrophobic metal salts, have been found to preferentially accumulate within the SMA template [13]. Pyrrole is a small, heterocyclic, non-polar molecule which is insoluble in water. By dissolving SMA at 1% wt/wt in neutral water, pyrrole was found to dissolve within the hydrophobic domains of SMA nanostructures suspended in aqueous solution. In time, a colour change indicated a reaction had occurred within the solution: pyrrole had polymerized into polypyrrole [14]. Following the polymerization by UV/vis showed the growth of a peak that red-shifted from 310nm to 480nm in proportion to polymer length.

Pyrrole polymerization is not a spontaneous reaction in the bulk, nor in pure water. Density functional theory molecular modeling shows that dimerization requires 93.6 kJ/mol; it isn't until the hexamer is reached that the polymer is favoured (by -191.6kJ/mol) over an equal number of independent monomers [14]. Two experiments were made to distinguish between the effects of physical

confinement and the interior chemistry of SMA22. First, the reaction was attempted in 1% solution of poly(isobutylene-*alt*-maleic acid), IMA. Like SMA, this polymer also self-assembles into a bi-layer sheet with a 2nm hydrophobic interior space in neutral water [15]. Pyrrole was found to spontaneously polymerize in this system in the same manner as in SMA solution. Second, a block copolymer polystyrene-*b*-poly(acrylic acid), PS-*b*-PAA, was used to produce 50nm micelles whose internal and external surfaces were chemically equivalent to those of SMA. Pyrrole was found to solubilize into the interior spaces of the micelles, but no polymerization occurred [14].

In the case of Platinum(II) chloride, it was found that the SMA template would also promote the reductant-free synthesis of mono-disperse platinum nanocrystals [13]. The reduction of platinum chloride to platinum metal without a reducing agent had never before been reported. The pyrrole polymerization experiment was repeated using platinum nanoparticle loaded SMA structures. Not only was the reaction rate increased by a factor of three, but the polypyrrole peak under UV/vis spectroscopy became sharper [13]. Since absorbance by polypyrrole is dependent on polymer length, the sharper peak indicates an increase in the frequency of occurrence of a particular chain length.

The confinement effect is thought to be a consequence of surface effects on local water phases. Since the mobility of the SMA structure is much lower than a water molecule, those water molecules that bond to the surface must lose velocity and, subsequently, kinetic energy. Since the water within the hydrophobic space is free to move (in fact much more free to move than bulk water due to the lack of restrictive hydrogen bonds [8]), the velocity of internal water molecules would increase in proportion to the energy lost from the frozen surface waters. The low water density and high velocity produces a supercritical phase of water within the SMA confinement space [8,16].

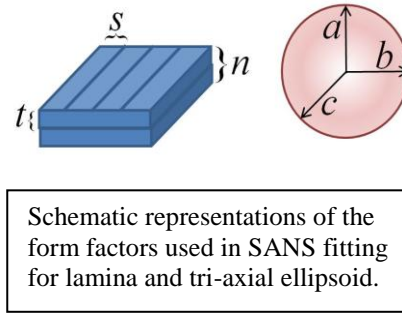
Pyrrole's hydrophobicity implies that its interaction with water is negligible and so would experience the potential energy field produced by external surface water as a curvature in the space that produces an apparent inward acceleration, i.e. compression, as observed. There is also a growing body of literature describing the formation of very small, monodisperse crystals in supercritical water [17], explaining the synthesis and morphology of the platinum nanocrystals previously observed.

3.2 Platinum in SMA solution

TEM images in the original study of platinum nanocrystal synthesis in SMA showed the crystals embedded within the polymer structure [13]. Investigation of the metal - polymer interactions are therefore important to establish the thermodynamically favoured site for platinum bonding and crystal nucleation. Density functional theory modeling was completed to probe the most stable geometries of ideal systems. A test platinum atom placed equidistant from the styrene (hydrophobic interior) and

Table 1. SANS model fitting parameters.

| | Parameter | SMA-Au pH7 | SMA-Pt pH7 | SMA-Pt pH5 |
|-----------|-------------------------------|------------|------------|------------|
| Lamina | SLD _{solid} | 1.87e-06 | 1.87e-06 | 1.87e-06 |
| | SLD _{solv} | 6.38e-06 | 6.38e-06 | 6.38e-06 |
| | Spacing s (Å) | 8.04 | 6.66 | 6.30 |
| | Thickness t (Å) | 95.64 | 14.59 | 12.61 |
| | Layers n (N) | 7.23 | 1.01 | 5.38 |
| Ellipsoid | SLD _{solid} | 4.66e-06 | 6.34e-06 | 6.34e-06 |
| | SLD _{solv} | 6.38e-06 | 1.87e-06 | 1.87e-06 |
| | Radius a (Å) | 2.68 | 16.76 | 7.97 |
| | Radius b (Å) | 162.04 | 7.87 | 14.61 |
| | Radius c (Å) | 266.78 | 13.69 | 14.74 |
| | Quality of fit (χ^2/n) | 3.749 | 18.483 | 85.763 |



maleic acid (hydrophilic exterior) moieties optimized to form bonds with two carbons of the styrene ring. The thermodynamic stability granted by this decrease in system energy indicates that the platinum - styrene bond is likely to be the nucleation site for crystal formation. This confirms that the clusters are embedded within the SMA interior hydrophobic spaces and corresponds with the 3nm limit of nanocrystal growth observed in TEM images.

To characterize the Pt-SMA system unsupported in aqueous solution, small angle neutron scattering (SANS) experiments were performed. SANS spectra give the intensity of q which, as a reciprocal of length, depicts the presence of smaller objects in its higher range. Further analysis is completed by fitting a function $P(q)$ to the intensity curve whose parameters precisely relate to the shape and dimensions of suspended materials.

The form factor used in the current study is a combination of a term to model the lamellar nanostructure of the SMA and a second term triaxial ellipsoid model to describe the scattering behaviour of the metal nanocrystals:

$$P(q) = 2\pi(\Delta\rho)^2\Gamma_m \frac{P_{bil}(q)}{q^2} Z_n(q) + \frac{scale}{V_{ell}} \int_0^1 \int_0^1 \phi^2 \left\{ q \left[a^2 \cos^2 \left(\frac{\pi x}{2} \right) + b \sin^2 \left(\frac{\pi x}{2} \right) (1 - y^2) + c^2 y^2 \right] \right\} dx dy$$

where

$$P_{bil}(q) = \left(\frac{\sin \left(\frac{qt}{2} \right)}{\frac{qt}{2}} \right)^2$$

$$\phi^2(x) = 9 \left(\frac{\sin x - x \cos x}{x^3} \right)^2$$

$Z_n(q)$ accounts for interference from n layers, and a , b , and c describe the radius of the three particle axes.

This model was applied to the Pt-SMA system at pH 5 and pH 7. The parameters used to produce best fit are listed in Table 1. The average diameter of nanocrystals in both samples is 2.5 nm, in good agreement with the previous study [13].

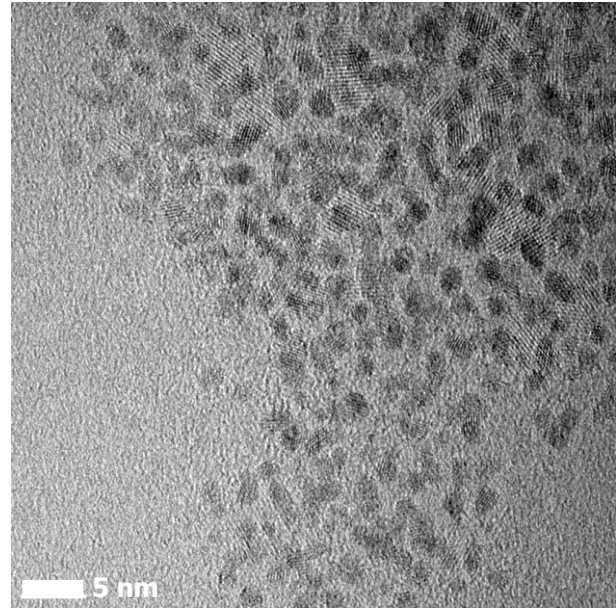


Figure 1: TEM image of platinum nanocrystals (dark circles) and lamellar SMA structure (hatched areas) at pH 5. Scale is 5nm.

3.3 Gold in SMA solution

Given the success and reliability of the platinum nanocrystal synthesis in SMA solution, the method was expanded to gold(I) chloride. While gold is generally inert and poor bulk catalyst, nanocrystalline gold demonstrates high catalytic reactivity for oxidation reactions [18]. As with platinum, the investigation into the reaction began with molecular modeling. Unlike platinum, however, DFT

simulation showed that the reduced gold atom preferentially interacts with the hydrophilic maleic anhydride group, meaning that crystal formation may occur on the outer surface of the SMA nanostructure.

The same lamina - ellipsoid model described above was applied to SANS data for the Au-SMA system. The radial parameters that describe the metal particles fit where one dimension is atomically thin (2.68 Å) and the others are quite broad (16.2 and 26.6 nm). Furthermore, the solvent adjacent to the gold is not SMA, as in the platinum sample, but D₂O. The parameters used to fit the model to SANS data are listed in Table 1.

TEM confirms the gold crystal morphology described by the SANS data. Images reveal atomically-thin gold nanosheets on the outer surface of the SMA lamina, shown in Figure 2. The regular and consistent 120° corner angles give the nanosheets a distinctly hexagonal geometry.

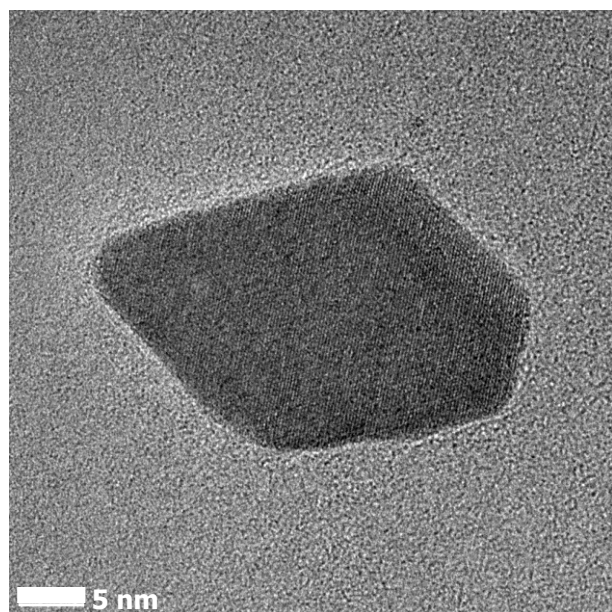


Figure 2: TEM micrograph of a single gold monolayer crystal. Scale is 5 nm.

4 CONCLUSION

Platinum(II) chloride will spontaneously concentrate within the hydrophobic spaces of SMA nanostructures to form monodisperse nanocrystals under 3 nm. The reaction is stable over a broad range of pH and the Pt-SMA nanoreactor it produces is likewise robust. Gold(I) chloride also spontaneously reduces in SMA solution but crystallizes on the surface of the structure rather than within it. These atomically thin hexagonal close-packing nanocrystals grow to hundreds of square nanometers in surface area and may initiate stacking of the Au-SMA system. The structure may then support confinement enhanced catalysis of hydrophilic oxidation reactions. Biomimetic metal-SMA nanoreactor systems hold great promise as tunable and versatile catalytic

agents for systems as diverse as carbon and nitrogen capture, proton exchange fuel cells, or water detoxification.

REFERENCES

- [1] D. Gust, T.A. Moore, and A.L. Moore, *Acc. Chem. Res.*, 42, 1890-1898, 2009.
- [2] A. Magnuson, M. Anderlund, O. Johansson, P. Lindblad et al. *Acc. Chem. Res.*, 42, 1899-09, 2009.
- [3] M. Müllner, T. Lunkenbein, M. Scheider, A.H. Gröschel et al. *Macromolecules*, 45, 6981-88, 2012.
- [4] J. Kang and J. Rebek Jr, *Nature*, 385, 50-52, 1997.
- [5] M. Raynal, P. Ballester, A. Vidal-Ferran, and P.W.N.M. Van Leeuwen, *Chem. Soc. Rev.*, 43, 1734-1787, 2014.
- [6] C. Malardier-Jugroot, T.G.M. Van de Ven, T. Cosgrove et al. *Langmuir*, 21, 10179-10187, 2005.
- [7] C. Malardier-Jugroot, T.G.M. Van de Ven, M. Whitehead. *J. Phys. Chem. B*, 109, 7022-7032, 2005.
- [8] M.E. Johnson, C. Malardier-Jugroot, R. Murarka et al. *J. Phys Chem. B*, 4082-4092, 2008.
- [9] G. Garnier, M. Duskova-Smrckova, R. Vyhalkova et al. *Langmuir*, 16, 3757-3763, 2000.
- [10] M. McTaggart, M. Jugroot, C. Malardier-Jugroot, *C. Chem. Phys. Lett.*, Submitted, 2015.
- [11] Gaussian 09, Rev. B.01, M.J. Frisch et al. Gaussian, Inc., Wallingford CT, 2009.
- [12] E.S. Kryachko, A.V. Arbuznikov, M.F.A. Hendrickx, *J. Phys. Chem. B*, 105, 3557-3566, 2001.
- [13] M.N. Groves, C. Malardier-Jugroot, and M. Jugroot, *Chem. Phys. Lett.*, 612, 309-312, 2014.
- [14] X. Li and C. Malardier-Jugroot, *Macromol*, 46, 2258-2266, 2013.
- [15] A.S.W. Chan, M. Groves, C. Malardier-Jugroot. *Mol. Simul.*, 37, 701-709, 2011.
- [16] A.J. Patel. *J. Phys. Chem. B.*, 1632-1637, 2010.
- [17] H. Hayashi, Y. Hakuta. *Materials (Basel)*, 3, 3794-3817, 2010.
- [18] T. Fujita, P. Guan, K. McKenna, X. Lang et al. *Nat. Mater.*, 11, 775-780, 2012.
- [19] X. Huang, S. Li, Y. Huang, S. Wu, X. Zhou et al. *Nat. Comms.*, 2, 292, 2011.